

Investigation of Aerodynamic Capabilities of Flying Fish in Gliding Flight

Hyungmin Park and Haecheon Choi*

School of Mechanical and Aerospace Engineering, Seoul National University, Seoul, Korea

**Corresponding author: choi@snu.ac.kr*

Abstract. In the present study, we experimentally investigate the aerodynamic capabilities of flying fish. We consider four different flying fish models, which are darkedged-wing flying fishes stuffed in actual gliding posture. Some morphological parameters of flying fish such as lateral dihedral angle of pectoral fins, incidence angles of pectoral and pelvic fins are considered to examine their effect on the aerodynamic performance. We directly measure the aerodynamic properties (lift, drag, and pitching moment) for different morphological parameters of flying fish models. For the present flying fish models, the maximum lift coefficient and lift-to-drag ratio are similar to those of medium-sized birds such as the vulture, nighthawk and petrel. The pectoral fins are found to enhance the lift-to-drag ratio and the longitudinal static stability of gliding flight. On the other hand, the lift coefficient and lift-to-drag ratio decrease with increasing lateral dihedral angle of pectoral fins.

Key words: flying fish, aerodynamic performance, gliding, static stability, wing morphology.

1. Introduction

Other than numerous birds and flying insects, several vertebrates have been observed to possess an ability to fly in air [1, 2]. Among them, marine flying fish has been noted for its excellent flight performance and a few early studies investigated the basic aerodynamics of flying-fish flight based on the field observations [3, 4, 5]. Morphologically the flying fish has hypertrophied pectoral and pelvic fins which it uses as wings for gliding flight. The flight of flying fish is quite remarkable, e.g., it can glide the distance over 400m in successive flights which are enabled by the unique method for take-off, named ‘taxiing’. Recently several biologists like Davenport [6, 7, 8] and Fish [9] conducted allometric studies in relation to the aerodynamic performance of flying fish. They measured the variations of morphometric parameters for various flying-fish species in live or preserved states and analyzed their influences on the flight characteristics.

Although several aspects of flying-fish flight has been understood or conjectured in previous studies, any quantitative analysis about the flying-fish flight has not been conducted so far. Furthermore, it might be interesting to compare the aerodynamic properties of flying-fish flight with those of other fliers in nature. Therefore, in the present study, we directly measure the aerodynamic forces and moment on flying-fish models in a wind tunnel. To meet the real flight

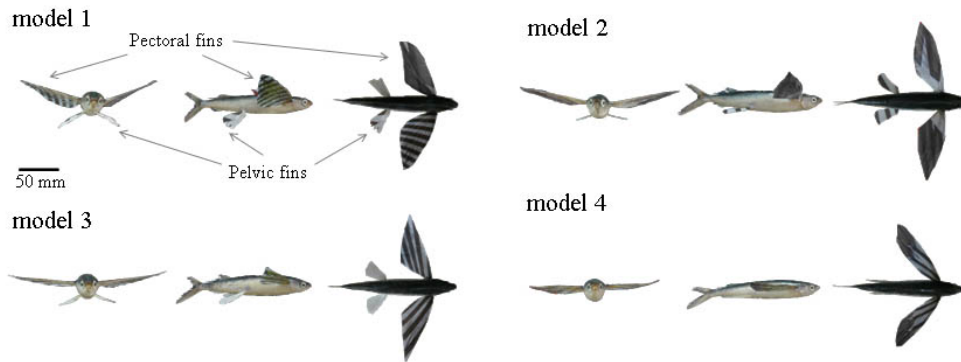


Figure 1. Pictures of the flying fish (*Cypselurus hiraii*) models considered in the present study.

condition of flying fish, flying-fish models are made of the real darkedged-wing flying fishes (*Cypselurus hiraii*) that are stuffed in gliding posture. The force measurements are conducted at the free-stream velocity of 12m/s. The maximum flight speed of real flying fish is known to be 10 ~ 20m/s [7, 9]. We also investigate the aerodynamic function of flying fish's wing morphology.

2. Experimental Setup

2.1. FLYING-FISH MODELS

For our study, we collected about forty darkedged-wing flying fish (*Cypselurus hiraii*) and stuffed four of them in appropriate gliding postures (Figure 1). As shown in Figure 1, *Cypselurus hiraii* has both enlarged pectoral and pelvic fins and we consider the wing configuration of each flying-fish model as follows: (a) both pectoral and pelvic fins enlarged (models 1 ~ 3), and (b) only pectoral fins enlarged with pelvic fins folded against the body (model 4).

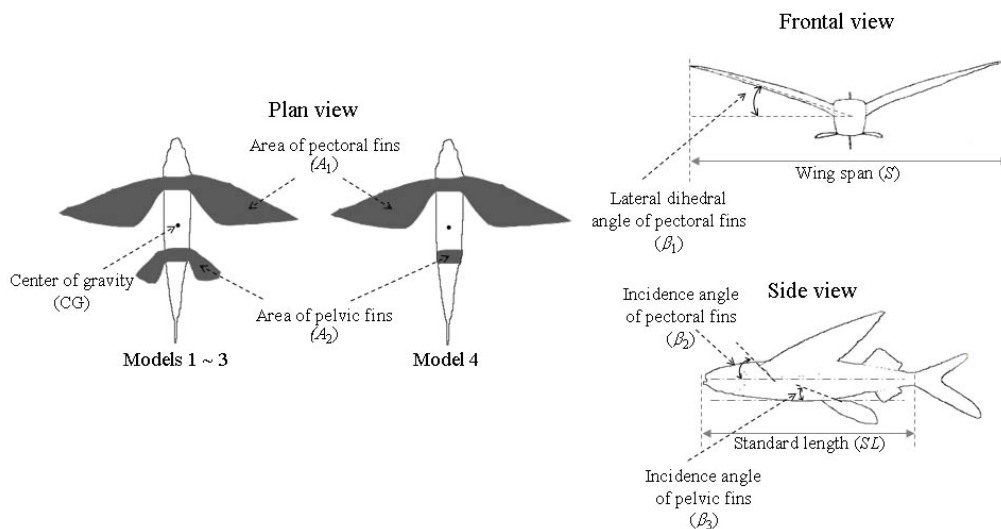


Figure 2. Definitions and orientations of morphometric parameters.

Table 1. Morphometric parameters of the flying fish models.

Models	1	2	3	4
Standard length (SL , mm)	205	209	203	199
Aspect ratio (AR)	8.5	9.1	9.8	9.6
Pectoral fin area (A_1 , mm ²)	7468	7392	6946	5639
Pelvic fin area (A_2 , mm ²)	1858	2020	2131	-
Wing span (S , mm)	252	260	261	233
Averaged chord length of pectoral fins (c , mm)	29.6	28.4	26.6	24.2
Lateral dihedral angle of pectoral fins (β_1 , degree)	22	12	7	5
Incidence angle of pectoral fins (β_2 , degree)	12	15	12	8
Incidence angle of pelvic fins (β_3 , degree)	2	2	5	-

For four models, we measured several parameters representing the aerial morphology of flying fish as tabulated in Table 1. Definitions of these parameters are illustrated in Figure 2. For models 1 ~ 3, the lateral dihedral angles (β_1) of pectoral fins are artificially changed such that models 1 and 3 have largest and smallest β_1 , respectively. On the other hand, other parameters are the original values of the specimen. The aspect ratio (AR) of the present flying fish is around 8.5 ~ 9.8 which is comparable to those of birds in general [2, 9]. Each flying-fish model is connected to the force/torque sensor to measure aerodynamic forces and moment.

2.2. FORCE MEASUREMENTS

Force measurements are performed in an open-circuit blowing-type low-speed wind tunnel as shown in Figure 3. Here, x , y , z denote the streamwise, vertical and spanwise directions, respectively. The test section has the size of 3m * 0.3m * 0.6m in the streamwise, vertical and spanwise directions, respectively and the maximum speed is 25m/s. At the free-stream velocity of 10m/s, the background turbulence intensity and the uniformity of the mean velocity is within 0.5%.

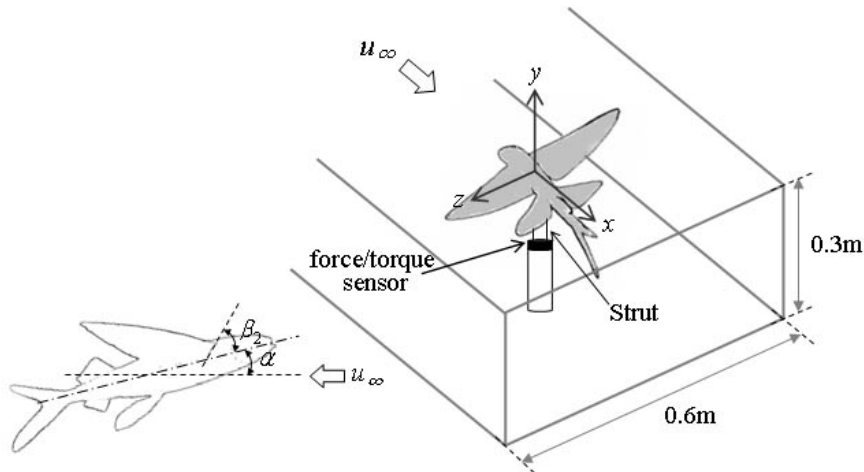


Figure 3. Schematic diagram of the force measurement in a wind tunnel.

To measure the forces and moment, we use a 6-axis force/torque sensor (NANO17, ATI) that measures 3-components of forces and moments simultaneously. The resolutions of the sensor are 1/1280N and 1/256Nmm in measuring force and moment, respectively. Varying the attack angle (α , see Figure 3) in the range of $-15^\circ < \alpha < 45^\circ$, we measure the lift and drag forces, and pitching moment for models 1 ~ 4. To minimize the interference by the strut, we use very slender strut whose cross section is an ellipse with maximum thickness is 2.68mm. The repeatability error of the measurement is within $\pm 1.5\%$. The raw signals from the sensor are digitized by the A/D converter (PXI-6259, NI) for 300 seconds at the sampling rate of 10kHz.

As the maximum flight speed of real flying fish has been reported to be 10 ~ 20m/s [7, 9], force measurement is conducted at the free-stream velocity (u_∞) of 12m/s and the corresponding Reynolds numbers are $Re = u_\infty c / \nu = 20,000 \sim 24,000$, where u_∞ is the free-stream velocity, c is the averaged chord length of the pectoral fins and ν is the kinematic viscosity.

3. Results and Discussion

From the measured lift (L), drag (D) and pitching moment (M), we obtain lift (C_L), drag (C_D) and pitching moment (C_M) coefficients as a function of angle of attack as follows:

$$C_L = L / (0.5\rho u_\infty^2 A). \quad (1)$$

$$C_D = D / (0.5\rho u_\infty^2 A). \quad (2)$$

$$C_M = M / (0.5\rho u_\infty^2 A_1 c). \quad (3)$$

where ρ is the density of air, and A is the total wing area, $A_1 + A_2$ (see Figure 2 and Table 1).

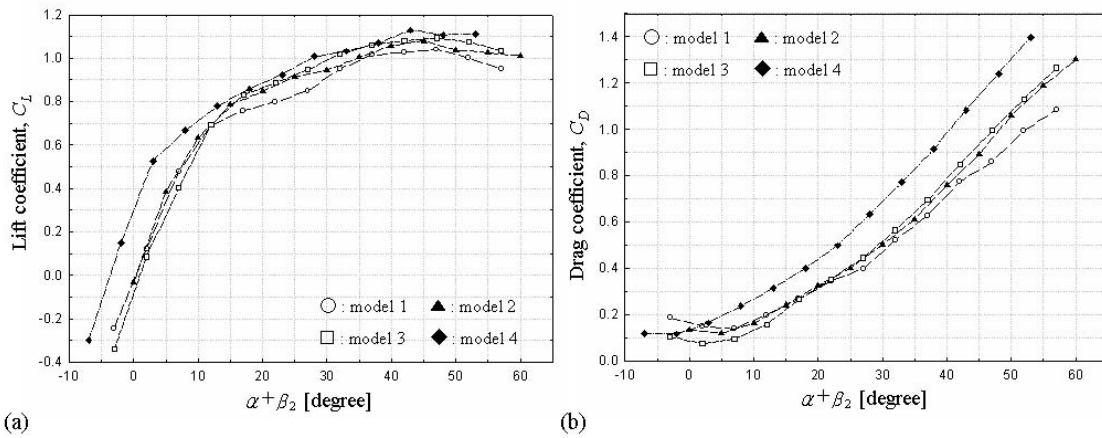


Figure 4. Variations of the lift (C_L) and drag (C_D) coefficients with the attack angle: (a) C_L ; (b) C_D .

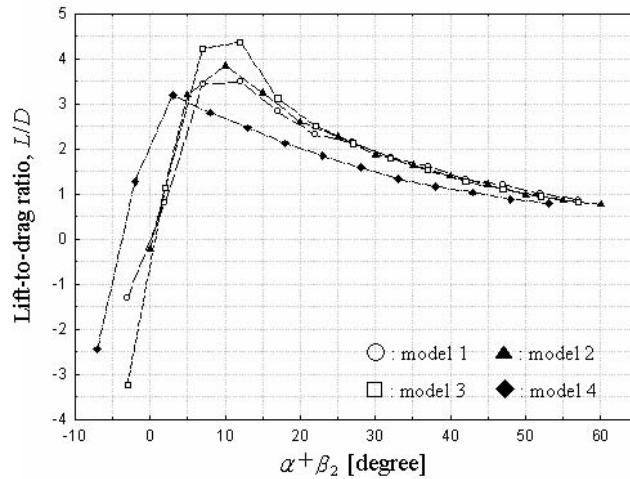


Figure 5. Variations of the lift-to-drag ratio (L/D) with the attack angle.

Figure 4 shows the variations of the lift and drag coefficients with respect to the attack angle, $\alpha + \beta_2$, for models 1 ~ 4. Here, β_2 is the incidence angle of the pectoral fins which is different for each model (Table 1). As shown in Figure 4, the maximum lift coefficients are about 1.0 ~ 1.1 and the minimum drag coefficients are about 0.07 ~ 0.12, which are similar to those of the vulture and nighthawk [10]. The lift coefficients for models 1 ~ 3 (with both enlarged pectoral and pelvic fins) are smaller than that of model 4 (with only pectoral fins enlarged). Since the area of the pelvic fins is about 20% of the total wing area (Table 1), pelvic fins do not enhance the wing loading. On the other hand, the lift coefficient decreases with increasing lateral dihedral angle of pectoral fins (β_1).

The variations of lift-to-drag ratio with the attack angle, $\alpha + \beta_2$ are given in Figure 5. The maximum lift-to-drag ratio is about 4.4 (model 3) which is greater than that of hawk (3.8) and petrel (4.0) [10]. The lift-to-drag ratios for models 1 ~ 3 are larger than that of model 4, indicating that the pelvic fins enhance the gliding performance of flying fish by having smaller drag coefficient. Like the lift coefficient, the lift-to-drag ratio also decreases with increasing lateral dihedral angle of pectoral fins (β_1).

For a gliding animal, flight stability is also one of the important issues. It is known that the nose-down pitching moment should increase with increasing attack angle (i.e., the slope of the pitching moment coefficient curve should be negative) for a glider to have a longitudinal static stability [11]. Also, the more negative the slope of pitching moment curve, the more stable the glider is. The variations of the pitching moment coefficient at the center of gravity are shown in Figure 6. It is found that the gliding flight of flying fish is statically stable in longitudinal direction, and with pelvic fins (models 1 ~ 3) the longitudinal static stability is enhanced, which is similar to the function of tail plane in modern aircraft. On the other hand, the longitudinal static stability is more enhanced with decreasing lateral dihedral angle of pectoral fins (β_1).

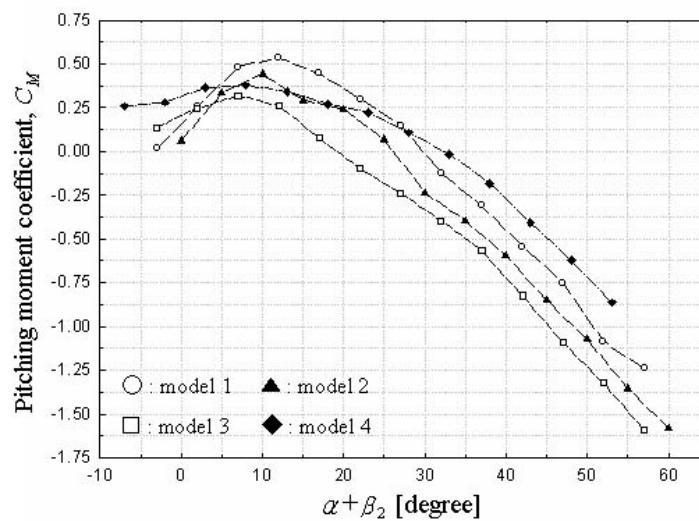


Figure 6. Variations of the pitching moment coefficient (C_M) with the attack angle.

4. Conclusions

In the present study, we investigated the aerodynamic properties of flying-fish flight by directly measuring the lift and drag forces, and pitching moment on real flying-fish models. The flying fish has a wing performance comparable to those of birds like the vulture, nighthawk and petrel in terms of the lift coefficient and lift-to-drag ratio. We also examined the effects of wing morphologies on the gliding performance of flying fish. Enlarged pelvic fins enhanced the lift-to-drag ratio and longitudinal static stability of the flying fish, but, the lift coefficient decreased due to enlarged pelvic fins. On the other hand, the lift coefficient and lift-to-drag ratio decreased with increasing lateral dihedral angle of pectoral fins.

Acknowledgements

This work has been supported by the National Research Laboratory Program of the Korean Ministry of Science and Technology.

References

1. Alexander, D.E., *Nature's Flyers*, The Johns Hopkins University Press (2002).
2. Vogel, S., *Lift in Moving Fluids*, Princeton University Press (1994).
3. Breder, C.M., Jr., On the structural specialization of flying fishes from the standpoint of aerodynamics. *Copeia* **4** (1930) 114–121.
4. Mills, C.A., Source of propulsive power used by flying fish. *Science* **83** (1936) 80.
5. Hertel, H., Take-off and flight of the flying fish. In: *Structure – Form – Movement*, eds. M.S. Katz, Reinhold Publishing Co, New York (1966) 218–224.

FLYING FISH IN GLIDING FLIGHT

6. Davenport, J., Wing-loading, stability and morphometric relationships in flying fish (Exocoetidae) from the north-eastern atlantic. *J. Mar. Biol. Ass. U. K.* **72** (1992) 25–39.
7. Davenport, J., How and why do flying fish fly? *Rev. Fish Biol. Fish.* **40** (1994) 184–214.
8. Davenport, J., Allometric constraints on stability and maximum size in flying fishes: implications for their evolution. *J. Fish Biol.* **62** (2003) 455–463.
9. Fish, F.E., Wing design and scaling of flying fish with regard to flight performance. *J. Zool., Lond.* **221** (1990) 391–403.
10. Withers, P.C., An aerodynamic analysis of bird wings as fixed aerofoils. *J. Exp. Biol.* **90** (1981) 143–162.
11. Thomas, A.L.R. and Taylor, G.K., Animal flight dynamics I. stability in gliding flight. *J. Theor. Biol.* **212** (2001) 399–424.